© 2014. Published by The Company of Biologists Ltd | Development (2014) 141, 4681-4689 doi:10.1242/dev.112029

RESEARCH ARTICLE

STEM CELLS AND REGENERATION

Transgenic analysis of a *SoxB* gene reveals neural progenitor cells in the cnidarian *Nematostella vectensis*

Gemma Sian Richards and Fabian Rentzsch*

ABSTRACT

Bilaterian neurogenesis is characterized by the generation of diverse neural cell types from dedicated neural stem/progenitor cells (NPCs). However, the evolutionary origin of NPCs is unclear, as neurogenesis in representatives of the bilaterian sister group, the Cnidaria, occurs via interstitial stem cells that also possess broader, non-neural, developmental potential. We address this question by analysing neurogenesis in an anthozoan cnidarian, *Nematostella vectensis*. Using a transgenic reporter line, we show that *NvSoxB(2)* – an orthologue of bilaterian *SoxB* genes that have conserved roles in neurogenesis – is expressed in a cell population that gives rise to sensory neurons, ganglion neurons and nematocytes: the three primary neural cell types of cnidarians. EdU labelling together with *in situ* hybridization, and within the *NvSoxB(2)::mOrange* transgenic line, demonstrates that cells express *NvSoxB(2)* before mitosis and identifies asymmetric behaviours of sibling cells within *NvSoxB(2)*$^+$ lineages. Morpholino-mediated gene knockdown of *NvSoxB(2)* blocks the formation of all three neural cell types, thereby identifying *NvSoxB(2)* as an essential positive regulator of nervous system development. Our results demonstrate that diverse neural cell types derive from an *NvSoxB(2)*-expressing population of mitotic cells in *Nematostella* and that *SoxB* genes are ancient components of a neurogenic program. To our knowledge this is the first description of a lineage-restricted, multipotent cell population outside the Bilateria and we propose that neurogenesis via dedicated, *SoxB*-expressing NPCs predates the split between cnidarians and bilaterians.

KEY WORDS: Cnidaria, Neurogenesis, Neural progenitor cells, *Nematostella*, *SoxB* genes

INTRODUCTION

The complex central nervous systems of bilaterians develop from a relatively small pool of multipotent neural progenitor cells (NPCs). These cells undergo a choreographed program of lineage expansion and diversification to generate an impressive number of specialized cell types in a strict spatio-temporal pattern. A characteristic feature of NPC development is the pattern of cell divisions within a lineage. Symmetric cell divisions can expand a progenitor pool or produce two terminally differentiated neurons, whereas asymmetric divisions produce unalike daughters with varying capacities for self-renewal or differentiation [reviewed by Huttner and Kosodo (2005)]. Well-studied examples, such as *Drosophila* neuroblasts and mammalian radial glial cells, demonstrate stereotypic lineage progressions, during which they take on distinct temporal identities and generate diverse daughter cells [reviewed by Kohwi and Doe (2013)]. The regulated differentiation of NPCs is thus considered part of the shared cellular framework of bilaterian neurogenesis. However, the evolutionary origin of NPCs is obscure, as a similar NPC-type population has not been identified in the bilaterian sister group, the Cnidaria (Fig. 1A).

Cnidarians (sea anemones, corals, jellyfish and hydroids) possess relatively simple nervous systems, consisting of sensory cells, ganglion cells (the morphological equivalent to interneurons) and nematocytes (stinging cells), which are usually considered to be a third, highly specialized, neural cell type [Fig. 1B; reviewed by Galliot et al. (2009)]. Although their neurons are not uniformly distributed, cnidarian polyps lack brain-like nervous system centralization and their nervous system is often described as a nerve net (Galliot et al., 2009; Watanabe et al., 2009). The cellular origin of neurons has mainly been described in hydrozoans (e.g. *Hydra*), in which a pluripotent, endodermally derived interstitial stem cell population gives rise to most neurons and nematocytes, as well as to gland cells and gametes (Bosch and David, 1987; Bosch, 2009; David, 2012; Müller et al., 2004). This origin of neurons differs significantly from bilaterian systems, but interstitial stem cells might represent a derived condition, as they have not been described outside hydrozoans.

The sea anemone *Nematostella vectensis* is an anthozoan cnidarian, and we have previously shown that its neurons derive from both germ layers, i.e. ectoderm and endoderm (Nakanishi et al., 2012). At the molecular level, *Nematostella* possesses many genes related to conserved bilaterian neural genes (Putnam et al., 2007; Watanabe et al., 2009), and subsets of its nervous system have been examined using antibodies against conserved neuropeptide precursor molecules [e.g. Marlow et al. (2009)]. The generation of neurons in *Nematostella* has previously been examined through studies of conserved bilaterian transcription factors. However, whereas many of these genes display evocative 'salt-and-pepper' expression patterns, and, in the case of the proneural orthologue *NvAshA*, can regulate the expression of putative neural markers (Layden et al., 2012), thus far none of these expression patterns has been definitively linked to the production of a mature neural cell type [e.g. Marlow et al. (2009); Matus et al. (2007a)]. Here, we address the developmental origins of neural cell types in anthozoans by employing a transgenic approach based on the putative neural regulator *NvSoxB(2)* (Magie et al., 2005).

NvSoxB(2) [also known as *SoxB2*, see Magie et al. (2005); *NveSoxBa*, see Royo et al. (2011)] is one of five *Nematostella* genes closely related to the bilaterian HMG-box-containing SoxB transcription factor family. The five *Nematostella SoxB* genes are expressed in overlapping patterns during embryogenesis, with *NvSoxB(2)* being expressed in a scattered pattern of individual cells in the ectoderm and endoderm (Magie et al., 2005) that is coincident with the timing of neurogenesis in these layers. In bilaterians, *SoxB* genes are expressed in the neural primordia of diverse organisms

Sars Centre for Marine Molecular Biology, University of Bergen, Thormøhlensgate 55, Bergen N-5008, Norway.

*Author for correspondence (fabian.rentzsch@sars.uib.no)

Received 30 April 2014; Accepted 23 September 2014

Development (2014) 141, 4681-4689 doi:10.1242/dev.112029

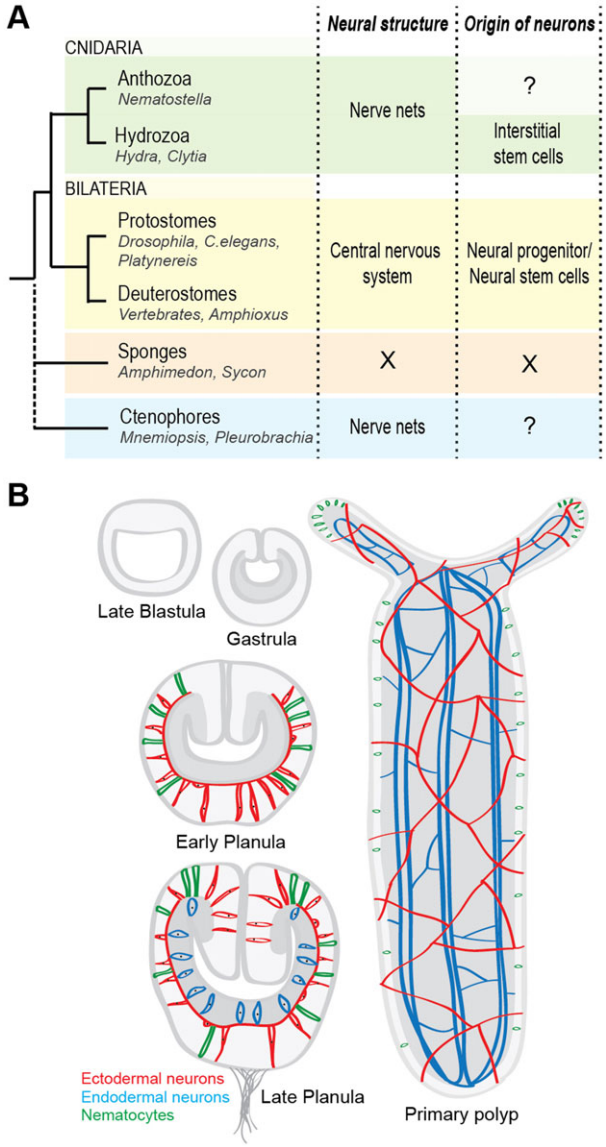

Fig. 1. An introduction to nervous system evolution in the animal kingdom and *Nematostella* neurogenesis. (A) Various grades of nervous system organization are present in the animal kingdom. Cnidarians possess multiple neural cell types that are assembled in basi-epithelial ectodermal and endodermal nerve nets, which can be considered as an intermediary stage between the non-neural sponges and bilaterians with complex centralized nervous systems. Bilaterian neurons derive from dedicated neural stem/progenitor cells, whereas in hydrozoans neurons originate from interstitial stem cells with broad development potential. In anthozoans, the cellular origin of neurons has not been described. The phylogenetic position of ctenophores remains controversial (dashed line) [e.g. Philippe et al. (2009); Ryan et al. (2013)] and, although they possess a nervous system, the precise ontogeny of their neural cells is unknown. (B) *Nematostella* develops from a hollow blastula into a bilayered gastrula via invagination at the animal pole. Differentiating ectodermal sensory neurons, ganglion neurons and nematocytes appear in early planulae. In later planulae, endodermal neurogenesis commences, with many of these neurons later condensing into longitudinal tracts which align to the developing musculature of the primary polyp. Diagrams are not to scale; all stages have oral pole up and show lateral cross-sections, except for the polyp, which depicts a section across the mesoglea (extracellular matrix separating ecto- from endoderm) showing both nerve nets. Light grey, ectoderm; dark grey, endoderm.

[e.g. polychaetes (Kerner et al., 2009), *Drosophila* (Buescher et al., 2002) and vertebrates (Bylund et al., 2003)]; across these organisms, *SoxB* genes are commonly expressed transiently in NPCs and are downregulated prior to terminal differentiation. Based on sequence similarity, bilaterian *SoxB* genes have been classed into two groups, *SoxB1* and *SoxB2*, although phylogenies commonly only resolve a monophyletic *SoxB1* group, which resides within an unresolved group of the other *SoxB* genes [designated *SoxB2*, see Bowles et al. (2000); Jager et al. (2011); Wilson and Dearden (2008)]. The precise phylogenetic affinities of cnidarian *SoxB* genes are currently uncertain [e.g. Jager et al. (2011)].

Thus far, functional studies of *SoxB* genes have been limited to investigations in classic model organisms. In vertebrates, *SoxB1* genes have an important role in the maintenance of NPCs (Bylund et al., 2003; Graham et al., 2003; Kishi et al., 2000). The best-described example is the chick neural tube, in which *SoxB1* genes (*Sox1-3*) suppress neurogenesis by maintaining neuroepithelial cells in an undifferentiated state, and *SoxB2* genes (*Sox21*, *Sox14*) promote neuronal differentiation by counteracting SoxB1 activity (Bylund et al., 2003; Graham et al., 2003; Holmberg et al., 2008; Sandberg et al., 2005). In *Drosophila*, functional studies have focused on two *SoxB* genes, *soxNeuro* (a *SoxB1* gene) and *dichaete* (probably a *SoxB2* gene), that are expressed in the neuroectoderm and are involved in the formation of neuroblasts (Buescher et al., 2002; Overton et al., 2007; Zhao and Skeath, 2002). However, their modes of activity do not bear direct comparison to vertebrate *SoxB1* and *SoxB2* genes, as both genes can positively regulate neural development by promoting neuroblast formation.

In this study, we present an *NvSoxB(2)::mOrange* transgenic reporter line, which we use to investigate the origin of neural cells and the function of *NvSoxB(2)* during early neurogenesis in *Nematostella*. We find that *NvSoxB(2)*-expressing cells give rise to three major neural cell types: sensory cells, ganglion cells and nematocytes. Using 5-Ethynyl-2′-deoxyuridine (EdU) labelling, we show that *NvSoxB(2)*$^+$ cells are mitotic, and that there are asynchronies in the division of sibling cells in *NvSoxB(2)*$^+$ lineages, which might underpin the generation of neural cell type diversity. With knockdown experiments we demonstrate that *NvSoxB(2)* regulates development of the nervous system but not ectodermal patterning. Together, these observations reveal the existence of dedicated NPCs in an anthozoan cnidarian and identify *SoxB* activity as an ancient regulator of neural progenitor populations.

RESULTS

Neurons and nematocytes are generated from a pool of *NvSoxB(2)*$^+$ cells

NvSoxB(2) was initially classified as a *SoxB2* gene, but has subsequently been shown to be a *SoxB* gene that cannot be grouped into the B1 or B2 subfamilies [e.g. Jager et al. (2011); Shinzato et al. (2008)]. *NvSoxB(2)* is expressed in scattered cells from blastula stage on, first in the ectoderm and later also in the endoderm (Magie et al., 2005). To test whether *NvSoxB(2)*-expressing cells contribute to the nervous system, we generated a stable transgenic line [*NvSoxB(2)::mOrange*], in which a promoter region of *NvSoxB(2)* drives the expression of the fluorescent reporter mOrange (Renfer et al., 2010; Shaner et al., 2004). This technique allows the identification of *NvSoxB(2)*-expressing cells and their progeny via the expression and inheritance of the mOrange reporter protein. Co-labelling of transgenic embryos with probes for both *mOrange* and *NvSoxB(2)* mRNA demonstrated strong (ca. 75-85%) correspondence between the expression of the reporter gene and that of endogenous *NvSoxB(2)* (supplementary material Fig. S1). Although we cannot unequivocally exclude that a specific sub-population of *NvSoxB(2)*-expressing cells is not represented in the transgenic line, we did not observe anything

Development (2014) 141, 4681-4689 doi:10.1242/dev.112029

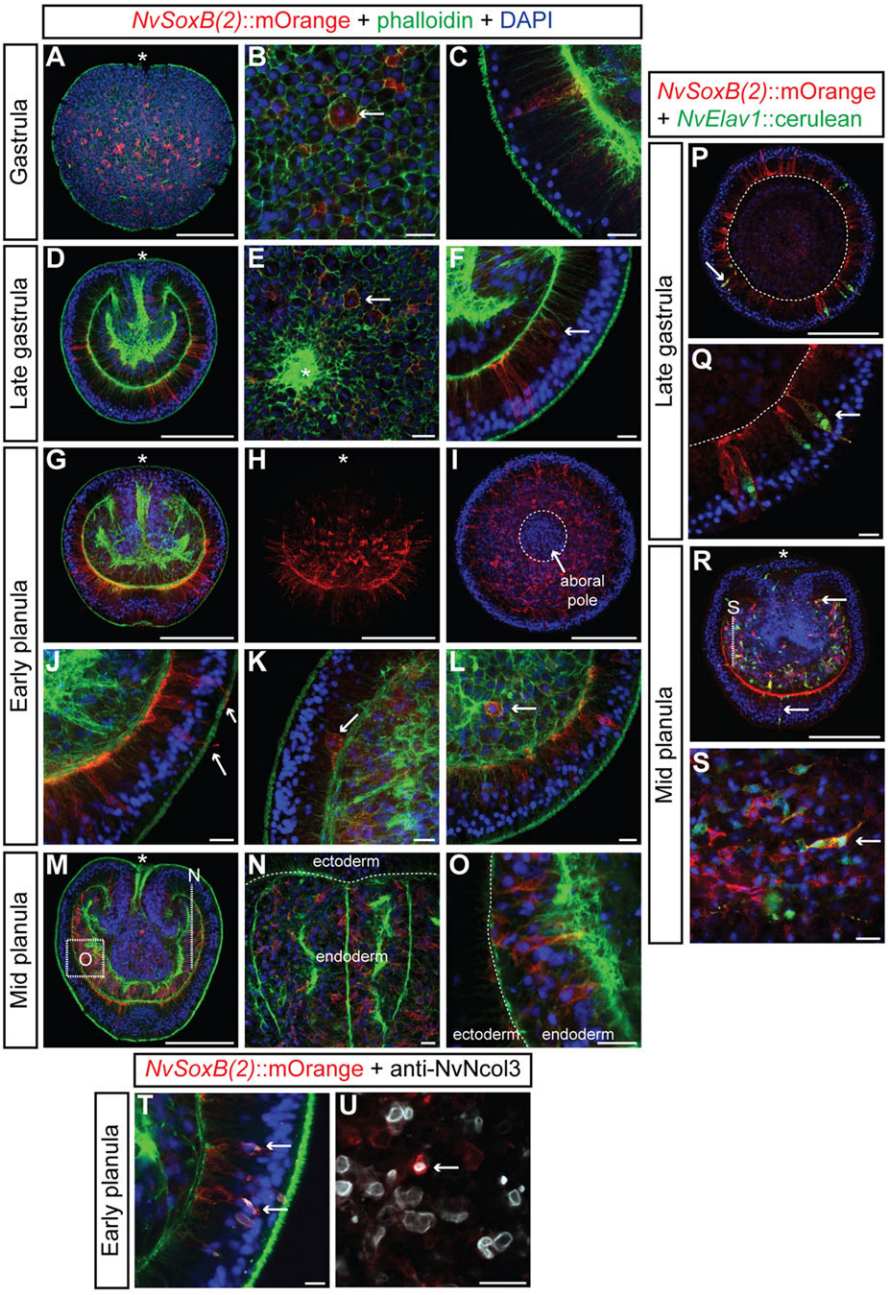

Fig. 2. The *NvSoxB(2)* promoter drives mOrange expression in cells of the developing nervous system. In gastrulae (A-F), mOrange is present in many ectodermal cells, some of which are dividing (arrows in B,E). By late gastrula, the differentiation of mOrange$^+$ ganglion cells is evident by their more basally located cell body (e.g. arrows in F,K). In early planula, many mOrange$^+$ cells have developed basal processes, forming the ectodermal nerve net (G-I); many of these cells are ciliated (arrows in J). Cells in the endoderm also begin to express mOrange (arrow in L). By mid-planula, many cells in the endoderm are positive for mOrange (M-O). Some of the mOrange$^+$ cells are positive for *NvElav1::cerulean*, in the ectoderm (arrows in P,Q) and endoderm (arrows in R,S). Others contain nematocysts, as labelled by anti-NvNcol3 (white) (arrows in T,U). (A,D,G,M,R) Lateral medial cross-sections, whole embryos; (C,F,J,K,O,Q,T) lateral medial cross-sections, higher magnification; (B,E,U) surface views/superficial sections; (I,P) aboral views; (L,N,S) sections through endoderm; (H,I) projections of half an embryo. Asterisks mark the oral pole. Dashed lines demarcate ectoderm and endoderm. Scale bars: 100 µm in A,D,G-I,M,P,R; 10 µm in all others.

that would support this suggestion – e.g. no systematic lack of colocalization of *NvSoxB(2)* and *mOrange* during a particular time point or in a particular region of the embryo. Subsequent analysis of reporter protein localization enabled us to identify that cells expressing *NvSoxB(2)* early in their development go on to become sensory, ganglion and nematocyte cells within the *Nematostella* ectodermal and endodermal nervous systems (Fig. 2; supplementary material Fig. S2).

In gastrula stages, mOrange is localized in scattered ectodermal cells – some are dividing at an apical position within the epithelium (Fig. 2A-F; Meyer et al., 2011). By early planula stage, mOrange localization highlights the development of the basi-epithelial ectodermal nerve net, located predominantly in the aboral two-thirds of the larva, but absent from directly under the aboral pole (where the larval apical organ is located; Fig. 2G-I). The nerve net is composed of neurites extending from the basal side of ectodermal neural cells; the primary orientation of these neurites is lateral, encircling the oral-aboral axis, but this is not strictly uniform (Fig. 2I). In addition to sensory neurons with medially located nuclei and apical cilia (Fig. 2J), *NvSoxB(2)::mOrange* also labels ganglion neurons, identified by their basal location in the ectoderm (Fig. 2K). In the early planula, activation of the *NvSoxB(2)* promoter becomes detectable in the endoderm (Fig. 2L). By mid-planula, mOrange is found in a large number of scattered cells throughout the endoderm, in addition to the ectodermal nerve net (Fig. 2M-O).

In later developmental stages, mOrange is localized in the ectodermal nerve net and in the ciliated neurons of the endodermal nervous system (supplementary material Fig. S2A-H). In primary polyps, mOrange localization highlights a close association between endodermal neurons and the longitudinal musculature, with bundles of neurites and cell bodies being aligned along the muscle fibres (supplementary material Fig. S2E-G).

Development (2014) 141, 4681-4689 doi:10.1242/dev.112029

In comparison to the previously characterized line *NvElav1::mOrange*, in which a promoter sequence of a marker of differentiated neurons drives mOrange expression in a subset of sensory and ganglion cells (Nakanishi et al., 2012), we found a greater number and diversity of cells labelled with mOrange in the *NvSoxB(2)* line (supplementary material Fig. S2I-L). In double-transgenic animals (*NvSoxB(2)::mOrange* × *NvElav1::cerulean*), the *NvElav1*$^{+}$ cell population is also labelled by the *NvSoxB(2)::mOrange* transgene (Fig. 2P-S). We speculated that *NvSoxB(2)*$^{+}$ cells that were *NvElav1*$^{-}$ might represent nematocytes, the third putative neural cell type of cnidarians. Thus, we performed an immunostaining on the *NvSoxB(2)::mOrange* line using an antibody against Minicollagen3 (NvNcol3), the major component of the capsule (nematocyst) of nematocytes (Zenkert et al., 2011). This experiment showed that a subset of the *NvSoxB(2)::mOrange* cells contained nematocysts, thus unambiguously identifying these cells as nematocytes (Fig. 2T,U). These data further support the classification of nematocytes as a bona fide neural cell type of cnidarians.

To better visualize the morphology and neurite projections of individual neurons we used a mosaic analysis based on the injection of an *NvSoxB(2)::EGFP* plasmid into eggs of the stable *NvSoxB(2)::mOrange* line (mosaicism of EGFP in the F0 population is due to spatio-temporal differences in construct incorporation/expression within and between embryos). These experiments confirmed the heterogeneity of the *NvSoxB(2)*$^{+}$ population, with regard to both cell shape and neurite projections arising from individual cells (supplementary material Fig. S2M-V). We found that *NvSoxB(2)*$^{+}$ cells are multipolar and that they display variation in the number, orientation, length and branching patterns of their basal projections. Variation is also apparent in the number and shape of varicosities found at the base of cells and along neurites. These observations hint at a considerable level of complexity in the neural architecture of this simple nerve net-based nervous system.

NvSoxB(2) is expressed in a scattered, proliferating cell population

Although the *NvSoxB(2)* transgenic line, through the inheritance of the stable reporter protein mOrange, reveals the contribution of *NvSoxB(2)*$^{+}$ cells to the three principal neural cell populations in *Nematostella*, it does not show when *NvSoxB(2)* is transcribed during the development of a neural cell. We thus extended the previous analysis of *NvSoxB(2)* transcription across a more detailed time course and tested for co-localization of *NvSoxB(2)* with neural differentiation markers. We found that the earliest expression of *NvSoxB(2)* is in the hollow coeloblastula, where it is expressed in discrete groups of cells distributed throughout the epithelium (Fig. 3A,J). The neural marker *anthoRFamide* [*NvRFamide*: sensory and ganglion neurons, Marlow et al. (2009)] is expressed in a few scattered single cells at this stage (Fig. 3D). By late blastula, the expression of *NvSoxB(2)*, *NvRFamide* and the nematocyte marker *minicollagen 3* [*NvNcol3*, Zenkert et al. (2011)], is in scattered single cells throughout the ectoderm (Fig. 3B,E,H), but fluorescent double *in situ* hybridization shows that there is no co-localization between *NvSoxB2* and either of the neural markers (Fig. 3L,N). In the gastrula, all three genes maintain scattered ectodermal expression patterns, with *NvSoxB(2)* being expressed in a greater number of cells (Fig. 3C,F,I). Again, we found no evidence for co-localization of *NvSoxB(2)* with *NvNcol3*; however, we observed some rare instances of co-localization with *NvRFamide* (Fig. 3M,O). By counter-staining for acetylated tubulin, we identified that some of the *NvSoxB(2)*-expressing cells possess a mitotic spindle and are thus undergoing cell division (also evidenced by their rounded shape and apical localization within

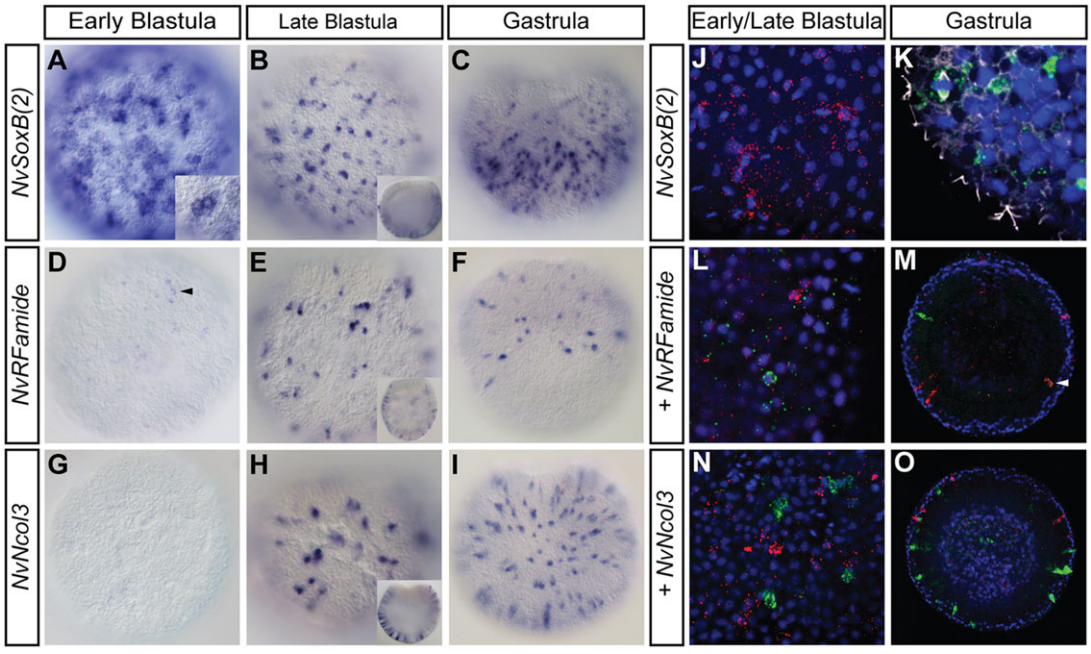

Fig. 3. *NvSoxB(2)* is expressed in proliferative ectodermal cells, but does not co-localize with markers of differentiating neural cells. In early blastulae, *NvSoxB(2)* is expressed in groups of cells (A,J), this resolves to a scattered single-cell pattern in late blastulae (B) and gastrula (C). (K) Some of these cells are dividing (green, *NvSoxB(2)*; white, anti-acetylated tubulin). The expression of markers for sensory neurons, *NvRFamide* (D-F), and for nematocytes, *NvNcol3* (G-I), is detected from early blastula and late blastula stages, respectively. There is limited overlap between *NvSoxB(2)* (red) and *NvRFamide* (green) expression (arrowhead in M), and no overlap between *NvSoxB(2)* (red) and *NvNcol3* (green) (L-O). (A-I) Surface views; insets in B,E,H, optical sections at mid-level. (J-O) Confocal images of FISH; blue, DAPI nuclear staining. (M-O) Whole embryo mid-sections. (J-L,N) Higher magnification of surface sections.

Development (2014) 141, 4681-4689 doi:10.1242/dev.112029

the ectodermal epithelium, Fig. 3K). At later stages, *NvSoxB(2)* expression continues to be seen in scattered ectodermal cells, some of which are dividing, and in the invaginating pharynx (supplementary material Fig. S3). Expression in endodermal cells is first detected in the early planula stage; a subset of these cells is also undergoing division (supplementary material Fig. S3).

Together with the transgenic analysis, these gene expression data suggest that *NvSoxB(2)* is transiently expressed in mitotically active cells that give rise predominantly or exclusively to neural cell types. This is in line with data from Bilateria, in which the timing of expression of *SoxB* genes is commonly restricted to specific phases of neurogenesis [e.g. Bylund et al. (2003); Kerner et al. (2009)].

Proliferating *NvSoxB(2)*$^+$ NPCs are present throughout development and in both germ layers

To further investigate proliferation within the *NvSoxB(2)*-expressing cell population, we incubated wild-type embryos for 30 min in the presence of the thymidine analogue EdU and then immediately fixed them for *in situ* hybridization with a probe for *NvSoxB(2)*. Note that, due to the relatively short EdU incubation period and the lack of a chase period prior to fixation, these data present only a snapshot of the total proliferation that will be occurring within the *NvSoxB(2)*$^+$ population. We have used this protocol to ensure that the cells labelled by EdU are those which are in a pre-mitotic state only. For analysis, we selected a 100 µm×100 µm area of ectoderm on the mid-lateral side of each of six embryos/stage and scored the number of *NvSoxB(2)*-expressing cells with and without EdU incorporation; we also estimated the total number of cells within the area (Fig. 4A-D). These experiments revealed that the number of *NvSoxB(2)*$^+$ cells in the sampled area remains relatively constant over the course of development, from early blastula to mid-planula. However, due to the increase in the total number of cells in the ectoderm during this time, the *NvSoxB(2)*$^+$ population makes up a larger proportion of the sampled ectoderm in earlier stages (e.g. compare 10% in early blastula with 2.5% in mid-planula). Similarly, whereas there is always a subset of *NvSoxB(2)*$^+$ cells incorporating EdU, this proportion is highest in early development and diminishes over time (e.g. compare 30% in early blastula with 10% in mid-planula). Overall, the level of EdU incorporation in the *NvSoxB(2)*$^+$ population is lower than that calculated for the rest of the ectoderm (supplementary material Fig. S4E). However, we cannot consider slow cell-cycling to be a definitive characteristic of the *NvSoxB(2)*$^+$ population, as our measure of cell proliferation in the rest of the ectoderm encompasses a mixture of cell types.

EdU labelling of *NvSoxB(2)::*mOrange$^+$ cells indicates asymmetries in sibling lineages

To examine cell division within the progeny of *NvSoxB(2)*$^+$ cells, we treated *NvSoxB(2)::mOrange* transgenic animals with a 30 min EdU pulse and fixed them immediately afterwards (Fig. 5A). As in the previous experiment, the mid-lateral ectoderm of embryos was examined. We scored for the presence of EdU incorporation in mOrange$^+$ cells and counted the number of contiguous mOrange$^+$ cells clustered around each EdU$^+$ mOrange$^+$ cell. As we did not observe expression of *NvSoxB(2)* mRNA in directly adjacent cells at the stages of analysis, we assume that contiguous transgenic cells predominantly represent sibling daughter cells produced via cell division of a common mother progenitor (supplementary material Fig. S5A). Notably, we recorded a range of differently sized mOrange$^+$ cell clusters (2-7 cells), indicating that mitoses of *NvSoxB(2)*$^+$ cells and their progeny can be asynchronous (synchronous cell division would result in even-numbered cell clusters only). As the majority of mOrange$^+$ cell clusters did not contain EdU$^+$ cells (a likely consequence of the short EdU incubation time, see note above), in the subsequent section we refer exclusively to clusters which contained at least one EdU$^+$ cell.

Within the mOrange$^+$ EdU$^+$ clusters, we commonly observed that only one cell was EdU positive, a further indication of asymmetries in the behaviours of sibling cells in the *NvSoxB(2)::mOrange* line. We next tested whether the cells in an EdU$^-$ cluster after the short incubation of 30 min would remain EdU$^-$ after a longer pulse. As the time from S phase to mitosis at gastrula stage is ca. 2-4 h (supplementary material Fig. S5B), we labelled gastrula stages with EdU for either 30 min or 2 h; a 2 h limit was chosen to ensure that EdU labelling captured pre-mitotic cells only. We further restricted our analysis to clusters containing 2-3 cells, as larger clusters might represent daughters from multiple founder cells, and we wanted to analyse sibling clones only. Our results show that, even when incubated with EdU for longer periods, in the majority of *NvSoxB(2)::mOrange*$^+$ two-cell clusters (97%) across both stages only one cell had incorporated EdU (Fig. 5B). Similarly, the number of cells labelled in the three-cell clusters did not change markedly between the two pulses within a stage; however, in early gastrulae a majority (90%) of three-cell clusters showed one EdU$^+$ cell, in contrast to two positive cells (73%) in gastrulae. Taken together, these findings identify differential cell cycling in the daughters of individual NPCs. Specifically, at a given time point, one daughter from an *NvSoxB(2)*$^+$ progenitor can be in S phase whereas the other is not. The cell not in S phase may be quiescent, post-mitotic or residing in

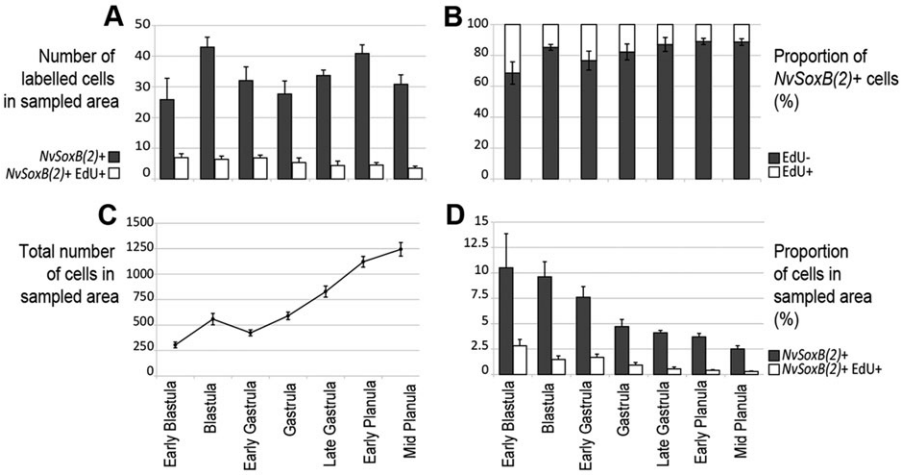

Fig. 4. EdU labelling reveals dynamics of *NvSoxB(2)*$^+$ cell proliferation during development. Over time, the number of cells expressing *NvSoxB(2)* in a 100 µm×100 µm patch of mid-lateral ectoderm remains roughly equivalent (A), with between 10% (mid-planula) to 25% (early blastula) of these cells also incorporating EdU (B). The total number of cells in the sampled area (C) increases from ~250 (early blastula) to ~1250 (mid-planula); thus, the relative proportion of cells expressing *NvSoxB(2)* within the ectoderm is ~fourfold higher in earlier stages (D). Average values from six embryos/stage; error bars: s.d.

Development (2014) 141, 4681-4689 doi:10.1242/dev.112029

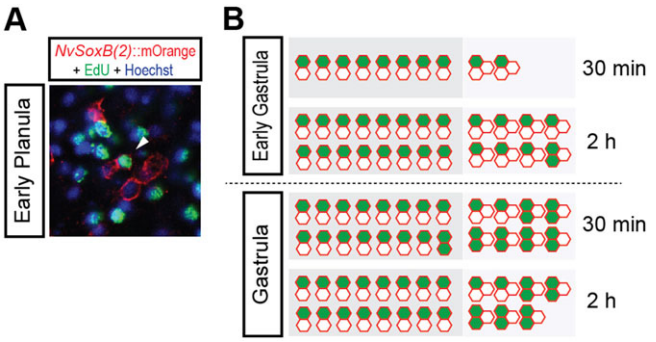

Fig. 5. Cell division is asynchronous in *NvSoxB(2)::mOrange*$^+$ lineages. (A) Incubation of *NvSoxB(2)::mOrange* transgenic embryos in EdU identifies S phase nuclei, and thus presumptive cell division events, within *NvSoxB(2)*$^+$ cells and their progeny (arrowhead). (B) In gastrula stages, within two-cell clusters, one cell is in S phase after a 30 min EdU pulse (23/24 clusters). After a 2 h pulse, it remains that only one cell per cluster is in S phase (32/32). In three-cell clusters, early gastrulae tend to show one labelled cell per cluster (9/10), whereas gastrulae display two per cluster (11/15); this pattern is unaffected by the length of EdU treatment. Data shown for each treatment are compiled from ten embryos/stage. EdU-incorporating cells, green; mOrange$^+$ cells, red.

G1/G2, with all of these cases representing asymmetry in the developmental progression of daughter cells from *NvSoxB(2)*$^+$ progenitors.

NvSoxB(2) regulates neurogenesis

To identify the function of *NvSoxB(2)*, we used a translation-inhibiting morpholino [*NvSoxB(2)*MO1] that targeted the 5′UTR of *NvSoxB(2)*. *NvSoxB(2)*MO1 caused a reduction in the expression of the neural markers *NvElav1*, *NvRFamide* and *NvNcol3* in the ectoderm of early planulae (Fig. 6A-F), but had no effect on the expression of the regional ectodermal markers *NvFkh*, *NvFGFa1* and *NvWnt2* (Fritzenwanker et al., 2004; Kusserow et al., 2005; Martindale et al., 2004; Matus et al., 2007b; Rentzsch et al., 2008; see also supplementary material Fig. S6H-M). Quantitative RT-PCR (RT-qPCR) confirmed that the expression of neural marker genes was decreased in *NvSoxB(2)* morphants, relative to control MO-injected embryos, at both the gastrula and planula stages (Fig. 6G). To determine the effect of this change in gene expression on the morphology of the larval nervous system, we assessed the presence of neurons and nematocytes in morphants by immunostaining against NvRFamide and NvNcol3, and by injecting the *NvSoxB(2)*MO1 into the *NvElav1*::*mOrange* transgenic line. In all cases, neural cells were strongly reduced or absent in the *NvSoxB(2)* morphants (Fig. 6H-P; for additional control experiments see supplementary material Fig. S6A-G). We conclude that *NvSoxB(2)* plays an important role in the development of three major neural cell types in *Nematostella*.

DISCUSSION

Together with observations in the *NvSoxB(2)::mOrange* transgenic line, our gene expression analyses suggest the existence of a population of dedicated NPCs in *Nematostella*. To our knowledge, this is the first description outside the Bilateria of a cell population restricted in fate (in this case neural) but able to generate multiple different cell types (i.e. sensory cells, ganglion cells and nematocytes). Our data are in contrast to studies on a different lineage of cnidarians, the Hydrozoa, in which neurons are mainly derived from pluripotent interstitial stem cells that give rise to both neural and non-neural cells (Bosch and David, 1987; Bosch, 2009; David, 2012; Muller et al., 2004). These observations suggest that *Nematostella* neural development is more akin to the epithelial progenitor-based neurogenesis of bilaterians than that of hydrozoans, although the levels and extent of homology between these processes remain to be analysed in detail. Indeed, with current data we cannot determine whether the NPCs of *Nematostella* and bilaterians are homologous, or whether they represent independent events of lineage restriction from an ancestral stem cell population which possessed broader, non-neural potential. Plasticity in the evolution of NPC lineages has previously been observed in the independent acquisition of neural stem cells in the arthropod and vertebrate lineages (Eriksson and Stollewerk, 2010).

By tracing the fate of *NvSoxB(2)*-expressing cells, we have revealed that sensory and ganglion neurons and nematocytes are linked via a common activation of the *NvSoxB(2)* promoter during their ontogeny (Fig. 7A). Following on from this discovery, it will be important to determine the potency of the *NvSoxB(2)*$^+$ population – whether it is homogenous [in that all *NvSoxB(2)*$^+$ cells have equal developmental potential] or whether it consists of multiple classes of neural progenitors that will go on to generate different numbers and types of neural cells (Fig. 7B). One possibility is that the NPC pool might be subdivided into nematocyte-producing cells and into cells that produce both sensory and ganglion neurons. Certainly at the molecular and morphological level, sensory and ganglion neurons have more in common with each other than either has with nematocytes [e.g. Marlow et al. (2009); Nakanishi et al. (2012)]. Such putative subsets of NPCs might in turn be defined by specific gene expression signatures, similar to the transcription factor coding of neural fate seen in bilaterian neurogenesis (Guillemot, 2007).

Intriguingly, our analysis of S phase labelling within sibling cells in the *NvSoxB(2)::mOrange* line demonstrated asymmetric cell behaviours within neural lineages of *Nematostella* (Fig. 5; supplementary material Fig. S5). In addition to identifying clusters of transgenic cells containing uneven cell numbers [most likely indicating asynchronous cell division from an initial *NvSoxB(2)*$^+$ progenitor], we observed that only one cell in a pair of sibling transgenic cells incorporated EdU, even after a period of prolonged EdU incubation. This probably indicates that either one of the two cells is already post-mitotic (G0), or that it is in an extended G1 phase and thus lagging behind the cell cycle of its sibling. These observations are noteworthy, as, both in mammals and *Drosophila*, changes in the length of cell cycle phases have been found to mark changes in the future trajectories of NPCs (Bayraktar et al., 2010; Bowman et al., 2008; Calegari et al., 2005; Takahashi et al., 1995). The cell cycle asymmetries we have documented in *Nematostella* might reflect differential self-renewal and/or the adoption of distinct fates by sibling cells within *NvSoxB(2)*$^+$ lineages. To understand the significance of these asymmetries, and their relationship to the generation of neural diversity in *Nematostella*, will require the application of live-imaging techniques and/or detailed clonal analysis, in combination with the development of an improved suite of neural cell type-specific markers.

An unexpected finding was that the absolute number of *NvSoxB(2)*$^+$ cells in our sampled area of ectoderm remained roughly the same from blastula to planula stage (Fig. 4). This could indicate that the *NvSoxB(2)*$^+$ population is a stable pool of stem cells residing in the ectoderm, from which differentiated neural cell types [no longer expressing *NvSoxB(2)*] emerge over time. Inconsistent with this scenario is that *NvSoxB(2)*$^+$ cells labelled with EdU generally display lower levels of *NvSoxB(2)* mRNA than other *NvSoxB(2)*-expressing cells. Furthermore, in the transgenic line we did not observe an accumulation of the reporter protein in cells labelled with

Development (2014) 141, 4681-4689 doi:10.1242/dev.112029

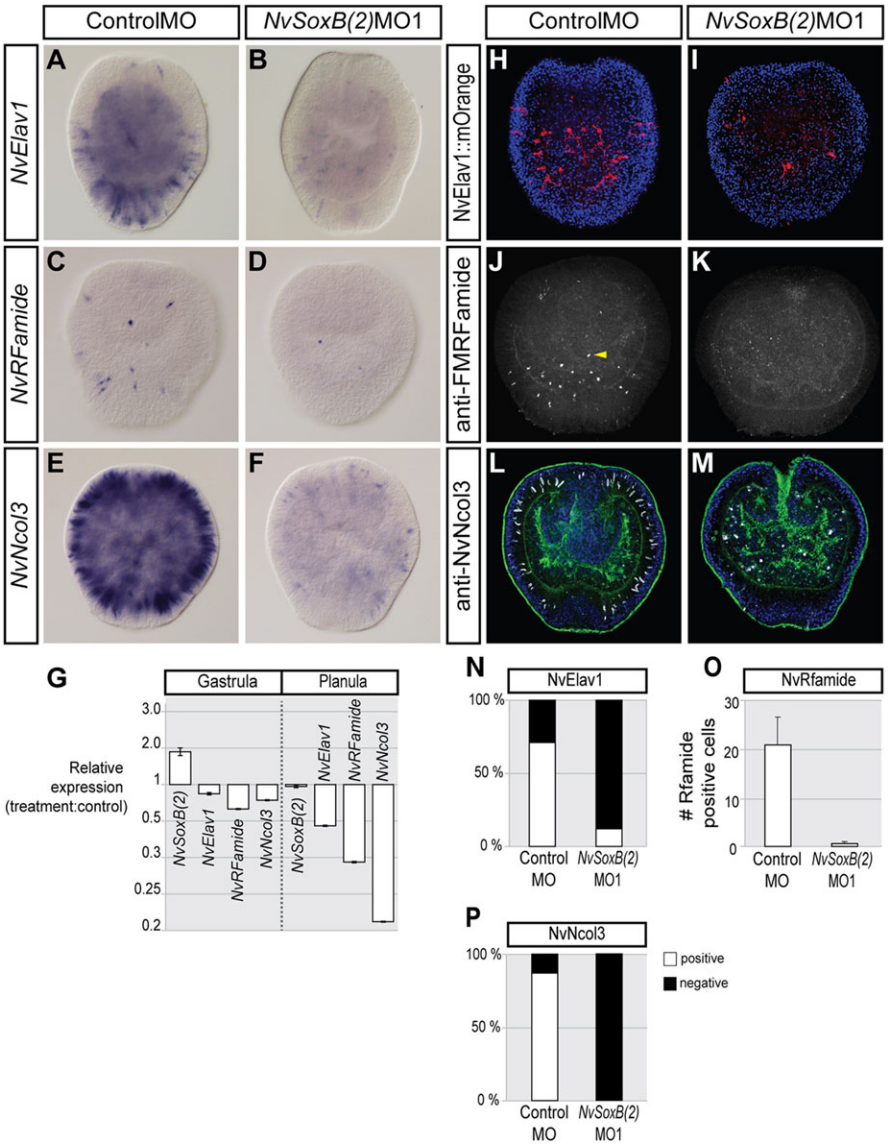

Fig. 6. Morpholino knockdown of *NvSoxB(2)* inhibits the expression of neural markers and the development of the nervous system. In *NvSoxB(2)* morphants, there is a reduction in expression of the neuron markers *NvElav1* (A,B) and *NvRFamide* (C,D) and of the nematocyte marker *NvNcol3* (E,F) at early planula stage. (G) RT-qPCR shows that this downregulation is evident in gastrulae, but more striking by planula stage. *NvElav1*::mOrange^{+} (red: H,I,N) and NvRFamide^{+} neurons (white: J,K,O), as well as NvNcol3^{+} nematocytes (white: L,M,P), do not develop in *NvSoxB(2)* morphants. (O,P) Embryos were scored 'positive' if displaying a wild-type pattern of immunostaining (Nakanishi et al., 2012; this study) and 'negative' if possessing few or no immunostained cells. *NvElav1::mOrange* animals are derived from an incross of a heterozygous line; thus, 25% of the animals are expected to be mOrange^{-}. *n*=28-41 in O; *n*=5 in P; *n*=12-15 in Q. All images have oral pole up. (A-F) *In situ* hybridizations; (H-M) immunostainings with DAPI (nuclei: blue) and phalloidin (F-actin: green). (A,B,E,F,L,M) Lateral cross-sections; (C,D) surface views; (H,K) projections of half an embryo.

EdU, as would be expected if this was a stable population of cells in which *NvSoxB(2)* was being continuously expressed. We therefore favour a scenario in which *NvSoxB(2)*$^{+}$ progenitors are constantly being produced, either from an unidentified pool of neural stem cells, or directly from ectodermal cells. In the latter case, their number could be kept constant over time by restrictive patterning mechanisms, such as lateral inhibition.

Among bilaterians there is no simple correlation between the orthology and function of specific *SoxB* family members. Similarly, in cnidarians *SoxB* genes can be expressed in stem cell populations and/or differentiating cells, in different neural cell types and at different developmental stages (Jager et al., 2011). This suggests that, whereas *SoxB* function in regulating the developmental progression of neural lineages has been conserved over evolutionary time, considerable variation has arisen in the specific roles that each family member might take during the course of neurogenesis.

The expression and functional data presented here indicate that *NvSoxB(2)* is required for the proper development of NPCs in *Nematostella*. *NvSoxB(2)* may either function as a positive regulator of NPC fate or act in the initiation of a neural differentiation program in an already formed NPC population. In the former scenario, we envisage that the broad expression of *NvSoxB(1)*, *NvSox1* and *NvSox3* (Magie et al., 2005) provides neural potential to ectodermal cells and that the scattered expression pattern of *NvSoxB(2)* is indicative of the promotion or stabilization of NPC fate. This scenario might further require that *NvSoxB(2)* be then downregulated for neural differentiation to proceed, akin to the requirement for *SoxB1* downregulation in the differentiation of the chick CNS (Bylund et al., 2003; Sandberg et al., 2005). The latter scenario, in which *NvSoxB(2)* promotes a neural differentiation program, resembles the function of the SoxB2 group gene *Sox21* in chick (Sandberg et al., 2005). *Sox21* counteracts the function of the SoxB1 group genes *Sox1*, *Sox2* and *Sox3*, which maintain NPCs in an undifferentiated state without promoting their proliferative activity (Bylund et al., 2003). Whether a similar antagonism between *SoxB* genes exists in *Nematostella* is unknown. The broad expression patterns of *NvSoxB(1)*, *NvSox1* and *NvSox3* are compatible with a role in maintaining an undifferentiated state that is counteracted by *NvSoxB(2)*, although they do not suggest a role that is specific to neural stem/progenitor cells. We thus favour the first scenario, in which *NvSoxB(2)* acts in the promotion/stabilization of NPC fate; however, more refined analyses will be required to determine the precise role of *NvSoxB(2)* in NPC generation and development.

Development (2014) 141, 4681-4689 doi:10.1242/dev.112029

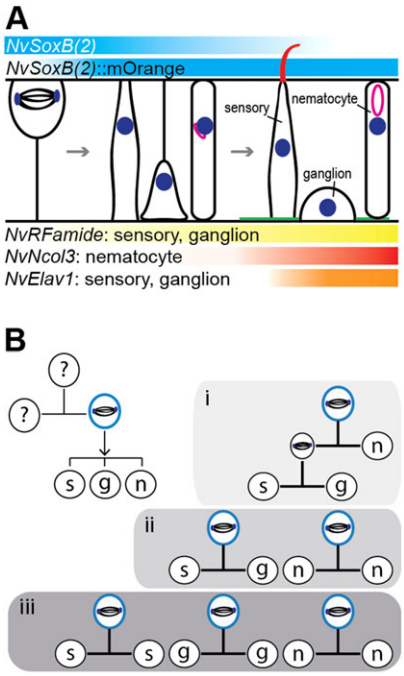

Fig. 7. Molecular and cellular characteristics of *Nematostella* neurogenesis. (A) *NvSoxB(2)* is expressed in proliferating NPCs that will go on to form sensory and ganglion neurons and nematocytes. These cell types can be distinguished (i) morphologically: by the localization of their nucleus, presence of basal extensions (green) and/or a sensory cilium (red) and presence of a nematocyst (pink); and (ii) genetically: by the expression of specific marker genes, e.g. *NvRFamide*, *NvElav1* and *NvNcol3*. (B) Three neural cell types are derived from a common *NvSoxB(2)*$^{+}$ progenitor population (blue). This study stimulates many questions regarding the origin of the *NvSoxB(2)*$^{+}$ cells (from stem cells or ectoderm) and the lineage of individual progenitors. *NvSoxB(2)*$^{+}$ NPCs might be (i) a homogenous multipotent population, with each cell capable of producing all three cell types; (ii) a heterogeneous population of neuron and nematocyte-specific progenitors; or (iii) a heterogeneous population of cell type-specific progenitors. s, sensory; g, ganglion; n, nematocyte.

In conclusion, we have identified *SoxB* genes as ancient genetic components of neurogenesis that are responsible for the regulation of NPC development. Our data further suggest that NPCs feature in the ground pattern of eumetazoan neurogenesis – in that cells destined for a neural fate enter an intermediary phase, whereby they can expand in number and generate an increased diversity of neural cell types via a combination of symmetric and asymmetric division. An improved understanding of the extent of molecular homology underpinning these processes in cnidarians and bilaterians will provide important insights into conserved core aspects of eumetazoan neural development and further illuminate the evolutionary plasticity of neurogenesis.

MATERIALS AND METHODS

Nematostella culture

Animals were maintained in 0.3× filtered seawater (NM) and induced to spawn as described by Fritzenwanker and Technau (2002). Fertilized eggs were removed from jelly packages by incubation for 25 min in 3% cysteine/NM. Embryos were raised at 21°C. Early blastula, 12 h; blastula, 16 h; late blastula, 18 h; early gastrula, 20 h; gastrula, 24 h; late gastrula, 30 h; early planula, 48 h; mid-planula, 72 h; late planula, 96 h; primary polyp, 10 days.

Transgenics

The *NvSoxB(2)::mOrange* transgenic line was generated by meganuclease-mediated transgenesis as described by Renfer et al. (2010). The *NvSoxB(2)* promoter sequence (genomic coordinates: minus strand on scaffold 84; 792,491-793,895) was cloned in front of mOrange (Shaner et al., 2004), with the addition of a membrane-tethering CAAX domain to help visualize the boundaries and morphology of cells expressing the reporter protein. Animals used for experiments were progeny from either incrossing of F1 heterozygotes or crossing F2 homozygotes with wild type. In all images, expression of mOrange was visualized via immunostaining with anti-DsRed (rabbit, Clontech, 632496; 1:100).

Morpholino injection

Microinjections were carried out as described by Rentzsch et al. (2008). Fertilized eggs were injected with 250-500 µM morpholino (Gene Tools) and 40 µg/ml Alexa Fluor-conjugated dextran (Invitrogen) in TAE buffer. Control injections used either a generic control or specific mismatch control [*NvSoxB(2)*Mm] morpholino. For morpholino sequences see supplementary material Table S2.

Fluorescent/*in situ* hybridization (FISH/ISH) and immunocytochemistry (ICC)

Experiments were conducted as described by Nakanishi et al. (2012) and Sinigaglia et al. (2013). For further details see supplementary material. Specimens were imaged on either a Nikon Eclipse E800 compound microscope with a Nikon Digital Sight DSU3 camera or on a Leica SP5 confocal microscope. Figure plates were built using Adobe Design Standard CS5; images were cropped and adjusted for brightness/contrast and colour balance; any adjustments were applied to the whole image, not parts.

Cell proliferation assays

Embryos were incubated with 100 µM EdU/DMSO in NM for either 30 min or 2 h at 21°C and then fixed (see methods in the supplementary material) immediately for either ICC or FISH. After ICC or FISH protocols were completed, EdU incorporation was visualized using the Click-iT EdU Alexa Fluor 488 imaging kit (Molecular Probes) following the manufacturer's instructions. For counting *NvSoxB(2)*$^{+}$ and EdU^{+} cells and cell clusters, a 100 µm×100 µm sampling area was defined in the mid-lateral region of the ectoderm, and serial 1 µm sections through the layer of nuclei within this region were scanned via confocal microscopy. For total cell number estimates, nuclei were counted within multiple 10 µm×10 µm subsamples of the 100 µm×100 µm region; these data were then extrapolated to the whole area.

RT-qPCR

RNA from embryos from three independent injections was extracted using the RNAqueous kit (Ambion) and DNAase-treated using TurboDNase (Ambion). Quality and quantity of RNA was assessed using a Bioanalyzer (Agilent). cDNA was reverse-transcribed using Superscript III (Invitrogen) primed with random hexamers (Roche). Control reactions without the addition of reverse transcriptase were prepared for all samples. Primer pairs with PCR efficiencies of 90-105% were used for qPCR. Two technical replicates were performed for each of the three biological replicates. Relative expression was calculated using the $2^{-\Delta\Delta Ct}$ method; control gene stabilities were assessed using RefFinder (http://www.leonxie.com), with *NvATPsynthase* and *NvELF1B* being selected as most stable. Mean relative expression and s.e.m. of three biological replicates are plotted. For primer sequences see supplementary material Table S1.

Acknowledgements

We thank Suat Özbek for generously providing the anti-Ncol3 antibody; Bård Steinar Giezendanner for animal care; Henriette Busengdal and Chiara Sinigaglia for advice on qPCR; and all S8 lab members for constructive discussions and experimental guidance.

Competing interests

The authors declare no competing financial interests.

Author contributions

F.R. generated the transgenic line and G.S.R. performed the experiments and analysis. Both authors contributed to the design of the study and the preparation of the manuscript.

Funding
Research in F.R.'s laboratory is supported by the Sars Centre core budget. G.S.R. was funded by a Marie Curie International Incoming Fellowship.

Supplementary material
Supplementary material available online at
http://dev.biologists.org/lookup/suppl/doi:10.1242/dev.112029/-/DC1

References

Bayraktar, O. A., Boone, J. Q., Drummond, M. L. and Doe, C. Q. (2010). Drosophila type II neuroblast lineages keep Prospero levels low to generate large clones that contribute to the adult brain central complex. *Neural Dev.* **5**, 26.
Bosch, T. C. G. (2009). Hydra and the evolution of stem cells. *BioEssays* **31**, 478-486.
Bosch, T. C. G. and David, C. N. (1987). Stem cells of Hydra magnipapillata can differentiate into somatic cells and germ line cells. *Dev. Biol.* **121**, 182-191.
Bowles, J., Schepers, G. and Koopman, P. (2000). Phylogeny of the SOX family of developmental transcription factors based on sequence and structural indicators. *Dev. Biol.* **227**, 239-255.
Bowman, S. K., Rolland, V., Betschinger, J., Kinsey, K. A., Emery, G. and Knoblich, J. A. (2008). The tumor suppressors Brat and Numb regulate transit-amplifying neuroblast lineages in Drosophila. *Dev. Cell* **14**, 535-546.
Buescher, M., Hing, F. and Chia, W. (2002). Formation of neuroblasts in the embryonic central nervous system of Drosophila melanogaster is controlled by SoxNeuro. *Development* **129**, 4193-4203.
Bylund, M., Andersson, E., Novitch, B. and Muhr, J. (2003). Vertebrate neurogenesis is counteracted by Sox1-3 activity. *Nat. Neurosci.* **6**, 1162-1168.
Calegari, F., Haubensak, W., Haffner, C. and Huttner, W. B. (2005). Selective lengthening of the cell cycle in the neurogenic subpopulation of neural progenitor cells during mouse brain development. *J. Neurosci.* **25**, 6533-6538.
David, C. N. (2012). Interstitial stem cells in Hydra: multipotency and decision-making. *Int. J. Dev. Biol.* **56**, 489-497.
Eriksson, B. J. and Stollewerk, A. (2010). Expression patterns of neural genes in Euperipatoides kanangrensis suggest divergent evolution of onychophoran and euarthropod neurogenesis. *Proc. Natl. Acad. Sci. USA* **107**, 22576-22581.
Fritzenwanker, J. and Technau, U. (2002). Induction of gametogenesis in the basal cnidarian Nematostella vectensis (Anthozoa). *Dev. Genes Evol.* **212**, 99-103.
Fritzenwanker, J. H., Saina, M. and Technau, U. (2004). Analysis of forkhead and snail expression reveals epithelial-mesenchymal transitions during embryonic and larval development of Nematostella vectensis. *Dev. Biol.* **275**, 389-402.
Galliot, B., Quiquand, M., Ghila, L., de Rosa, R., Miljkovic-Licina, M. and Chera, S. (2009). Origins of neurogenesis, a cnidarian view. *Dev. Biol.* **332**, 2-24.
Graham, V., Khudyakov, J., Ellis, P. and Pevny, L. (2003). SOX2 functions to maintain neural progenitor identity. *Neuron* **39**, 749-765.
Guillemot, F. (2007). Spatial and temporal specification of neural fates by transcription factor codes. *Development* **134**, 3771-3780.
Holmberg, J., Hansson, E., Malewicz, M., Sandberg, M., Perlmann, T., Lendahl, U. and Muhr, J. (2008). SoxB1 transcription factors and Notch signaling use distinct mechanisms to regulate proneural gene function and neural progenitor differentiation. *Development* **135**, 1843-1851.
Huttner, W. B. and Kosodo, Y. (2005). Symmetric versus asymmetric cell division during neurogenesis in the developing vertebrate central nervous system. *Curr. Opin. Cell Biol.* **17**, 648-657.
Jager, M., Quéinnec, E., Le Guyader, H. and Manuel, M. (2011). Multiple Sox genes are expressed in stem cells or in differentiating neuro-sensory cells in the hydrozoan Clytia hemisphaerica. *EvoDevo* **2**, 12.
Kerner, P., Simionato, E., Le Gouar, M. and Vervoort, M. (2009). Orthologs of key vertebrate neural genes are expressed during neurogenesis in the annelid Platynereis dumerilii. *Evol. Dev.* **11**, 513-524.
Kishi, M., Mizuseki, K., Sasai, N., Yamakazi, H., Shiota, K., Nakanishi, S. and Sasai, Y. (2000). Requirement of Sox2-mediated signaling for differentiation of early Xenopus neuroectoderm. *Development* **127**, 791-800.
Kohwi, M. and Doe, C. Q. (2013). Temporal fate specification and neural progenitor competence during development. *Nat. Rev. Neurosci.* **14**, 823-838.
Kusserow, A., Pang, K., Sturm, C., Hrouda, M., Lentfer, J., Schmidt, H. A., Technau, U., von Haeseler, A., Hobmayer, B., Martindale, M. Q. et al. (2005). Unexpected complexity of the Wnt gene family in a sea anemone. *Nature* **433**, 156-160.
Layden, M. J., Boekhout, M. and Martindale, M. Q. (2012). Nematostella vectensis achaete-scute homolog NvashA regulates embryonic ectodermal neurogenesis and represents an ancient component of the metazoan neural specification pathway. *Development* **139**, 1013-1022.
Magie, C. R., Pang, K. and Martindale, M. Q. (2005). Genomic inventory and expression of Sox and Fox genes in the cnidarian Nematostella vectensis. *Dev. Genes Evol.* **215**, 618-630.
Marlow, H. Q., Srivastava, M., Matus, D. Q., Rokhsar, D. and Martindale, M. Q. (2009). Anatomy and development of the nervous system of Nematostella vectensis, an anthozoan cnidarian. *Dev. Neurobiol.* **69**, 235-254.
Martindale, M., Pang, K. and Finnerty, J. (2004). Investigating the origins of triploblasty: 'mesodermal' gene expression in a diploblastic animal, the sea anemone Nematostella vectensis (phylum, Cnidaria; class, Anthozoa). *Development* **131**, 2463-2474.
Matus, D. Q., Pang, K., Daly, M. and Martindale, M. Q. (2007a). Expression of Pax gene family members in the anthozoan cnidarian, Nematostella vectensis. *Evol. Dev.* **9**, 25-38.
Matus, D. Q., Thomsen, G. H. and Martindale, M. Q. (2007b). FGF signaling in gastrulation and neural development in Nematostella vectensis, an anthozoan cnidarian. *Dev. Genes Evol.* **217**, 137-148.
Meyer, E. J., Ikmi, A. and Gibson, M. C. (2011). Interkinetic nuclear migration is a broadly conserved feature of cell division in pseudostratified epithelia. *Curr. Biol.* **21**, 485-491.
Müller, W. A., Teo, R. and Frank, U. (2004). Totipotent migratory stem cells in a hydroid. *Dev. Biol.* **275**, 215-224.
Nakanishi, N., Renfer, E., Technau, U. and Rentzsch, F. (2012). Nervous systems of the sea anemone Nematostella vectensis are generated by ectoderm and endoderm and shaped by distinct mechanisms. *Development* **139**, 347-357.
Overton, P. M., Chia, W. and Buescher, M. (2007). The Drosophila HMG-domain proteins SoxNeuro and Dichaete direct trichome formation via the activation of shavenbaby and the restriction of Wingless pathway activity. *Development* **134**, 2807-2813.
Philippe, H., Derelle, R., Lopez, P., Pick, K., Borchiellini, C., Boury-Esnault, N., Vacelet, J., Renard, E., Houliston, E., Quéinnec, E. et al. (2009). Phylogenomics revives traditional views on deep animal relationships. *Curr. Biol.* **19**, 706-712.
Putnam, N. H., Srivastava, M., Hellsten, U., Dirks, B., Chapman, J., Salamov, A., Terry, A., Shapiro, H., Lindquist, E., Kapitonov, V. V. et al. (2007). Sea anemone genome reveals ancestral eumetazoan gene repertoire and genomic organization. *Science* **317**, 86-94.
Renfer, E., Amon-Hassenzahl, A., Steinmetz, P. R. H. and Technau, U. (2010). A muscle-specific transgenic reporter line of the sea anemone, Nematostella vectensis. *Proc. Natl. Acad. Sci. USA* **107**, 104-108.
Rentzsch, F., Fritzenwanker, J. H., Scholz, C. B. and Technau, U. (2008). FGF signalling controls formation of the apical sensory organ in the cnidarian Nematostella vectensis. *Development* **135**, 1761-1769.
Royo, J. L., Maeso, I., Irimia, M., Gao, F., Peter, I. S., Lopes, C. S., D'Aniello, S., Casares, F., Davidson, E. H., Garcia-Fernández, J. et al. (2011). Transphyletic conservation of developmental regulatory state in animal evolution. *Proc. Natl. Acad. Sci. USA* **108**, 14186-14191.
Ryan, J. F., Pang, K., Schnitzler, C. E., Nguyen, A.-D., Moreland, R. T., Simmons, D. K., Koch, B. J., Francis, W. R., Havlak, P. et al.; **NISC Comparative Sequencing Program** (2013). The genome of the ctenophore Mnemiopsis leidyi and its implications for cell type evolution. *Science* **342**, 1242592.
Sandberg, M., Källström, M. and Muhr, J. (2005). Sox21 promotes the progression of vertebrate neurogenesis. *Nat. Neurosci.* **8**, 995-1001.
Shaner, N. C., Campbell, R. E., Steinbach, P. A., Giepmans, B. N. G., Palmer, A. E. and Tsien, R. Y. (2004). Improved monomeric red, orange and yellow fluorescent proteins derived from Discosoma sp. red fluorescent protein. *Nat. Biotechnol.* **22**, 1567-1572.
Shinzato, C., Iguchi, A., Hayward, D. C., Technau, U., Ball, E. E. and Miller, D. J. (2008). Sox genes in the coral Acropora millepora: divergent expression patterns reflect differences in developmental mechanisms within the Anthozoa. *BMC Evol. Biol.* **8**, 311.
Sinigaglia, C., Busengdal, H., Leclère, L., Technau, U. and Rentzsch, F. (2013). The bilaterian head patterning gene six3/6 controls aboral domain development in a cnidarian. *PLoS Biol.* **11**, e1001488.
Takahashi, T., Nowakowski, R. S. and Caviness, V. S. (1995). The cell cycle of the pseudostratified ventricular epithelium of the embryonic murine cerebral wall. *J. Neurosci.* **15**, 6046-6057.
Watanabe, H., Fujisawa, T. and Holstein, T. W. (2009). Cnidarians and the evolutionary origin of the nervous system. *Dev. Growth Differ.* **51**, 167-183.
Wilson, M. J. and Dearden, P. K. (2008). Evolution of the insect Sox genes. *BMC Evol. Biol.* **8**, 120.
Zenkert, C., Takahashi, T., Diesner, M.-O. and Özbek, S. (2011). Morphological and molecular analysis of the Nematostella vectensis cnidom. *PLoS ONE* **6**, e22725.
Zhao, G. and Skeath, J. (2002). The Sox-domain containing gene Dichaete/fish-hook acts in concert with vnd and ind to regulate cell fate in the Drosophila neuroectoderm. *Development* **129**, 1165-1174.